

Enhancement of Nonlinear Optical Effect in One-Dimensional Photonic Crystal Structures

Noriaki TSURUMACHI, Shoichi YAMASHITA, Norio MUROI, Takao FUJI, Toshiaki HATTORI
and Hiroki NAKATSUKA

Institute of Applied Physics, University of Tsukuba, Tsukuba, Ibaraki 305-8573, Japan

(Received April 23, 1999; accepted for publication August 20, 1999)

We observed the photonic band structure of one-dimensional photonic crystals using a white-light Michelson interferometer. In one-dimensional photonic crystals with a structural defect, there is a localized mode where the field is localized around the position of the defect. If the defect is made of nonlinear optical material, the effective nonlinearity of the photonic crystal is largely enhanced by the enhanced light intensity at the defect. In a one-dimensional photonic crystal with a defect, we observed a large enhancement of degenerate four-wave mixing efficiency. Since the total thickness of the whole structure is only a few micrometers, it was successfully used to form an optical phase-conjugated image.

KEYWORDS: one-dimensional photonic crystal, photonic band structure, localized mode, white-light Michelson interferometer, optical nonlinearity, absorption saturation, degenerate four-wave mixing, optical phase conjugation

1. Introduction

In recent years, much effort has been devoted to the study of photonic crystals after the formal similarity between the Schrodinger equation for electrons and the Maxwell equation for photons was clearly recognized.^{1–3)} They are expected as the stage of mutual quantum control of radiation field and matter, and the control of photon modes by photonic crystals may open up a key technology for future photonic devices. We can consider various types of photonic crystal structures, from one-dimensional to three-dimensional ones, depending on the target. Since low-power lasers are indispensable for high-density optical integrated circuits, one of the important goals is to develop a thresholdless laser where spontaneous emission is controlled and allowed only in a single optical mode in a three-dimensional photonic crystal.^{4,5)} Photonic crystal structures may also serve as sophisticated complex waveguides in optical integrated circuits.⁶⁾ In addition to micro-lasers and waveguides, we need nonlinear optical devices which operate at very low light power for future optical processing technology.^{7,8)} Therefore, the enhancement of optical nonlinearity by using photonic crystals is of utmost importance.

At present, it is not easy to fabricate three-dimensional photonic crystals with the desired structures, since the control of the dielectric constant with spatial precision higher than the wavelength of light is very difficult. In many applications, however, the control of laser beams is required where laser beams are close to plane waves. In this case we do not require three-dimensional photonic crystals, i.e., one-dimensional photonic crystals (1-D PCs) or dielectric multilayers are sufficient. Furthermore, for the enhancement of optical nonlinearities, the 1-D PC is the best candidate since the incident light field is fully coupled to the localized defect mode only in the 1-D PC. The 1-D PCs in this scheme can be fabricated simply by stacking thin films with desired optical properties.

The nonlinear Fabry-Perot etalons and microcavities can be considered as a kind of 1-D PC. Using these structures, many functions such as bistability, multistability and optical limiting have been predicted theoretically and observed experimentally.^{9–12)} In analogy to the dynamics of electrons in a crystal, the propagation of light waves in such a structure with

a periodically modulated dielectric constant is well addressed by using the concept of photonic crystals. In our previous paper, we analyzed the optical nonlinearity due to defect states in 1-D PCs.¹³⁾

In this study, we first observe the linear propagation of light waves through 1-D PCs using a white-light Michelson interferometer. Then, we introduce an absorptive structural defect at the center of the 1-D PC and observe the strong enhancement of three kinds of optical nonlinearities. They are absorption saturation, degenerate four-wave mixing and optical phase conjugation. The demonstration of the image reconstruction by optical phase conjugation is aimed at future image processing using low-power lasers such as diode lasers.

2. Linear Properties of One-Dimensional Photonic Crystals

We made 1-D PCs without defects and with a structural defect to investigate the optical properties in the linear regime. In the present study, the basic structure of the 1-D PCs is composed of quarter-wave stacks of two dielectrics with different refractive indices. A schematic of a 1-D PC without defects is shown in Fig. 1(a). Here, layers A and B are SiO₂ and TiO₂, with refractive indices of 1.46 and 2.35, respectively, and they are stacked by vacuum deposition on a glass substrate. The optical thickness of both layers A and B is 600 nm/4, and the total number of layers is 21. Figure 1(b) shows a schematic of the 1-D PC with a structural defect where the periodicity is disturbed only by the defect layer which is in the center of the stacks. In this case, the optical thickness of the center defect layer is 1.6 times those of the periodic layers. Since the total number of layers is the same as that of the 1-D PC without defects, 21, the period, N, of A and B bilayers on each side of the defect layer is 5. Figures 2(a) and 2(b) show the calculated transmission spectra using the method of characteristic matrices for 1-D PCs without defects and with a defect, respectively. In Fig. 2(a), we see a wide photonic band gap centered at 500 THz (600 nm) where light transmission is prohibited. In this region, there are no photon modes which propagate normally to the surfaces of the layers. On the other hand, there is a sharp transmission peak in Fig. 2(b) at 528 THz (568 nm) in the band gap, which is due to a defect level introduced by the defect layer.

The phase-sensitive observation of the electric field of light

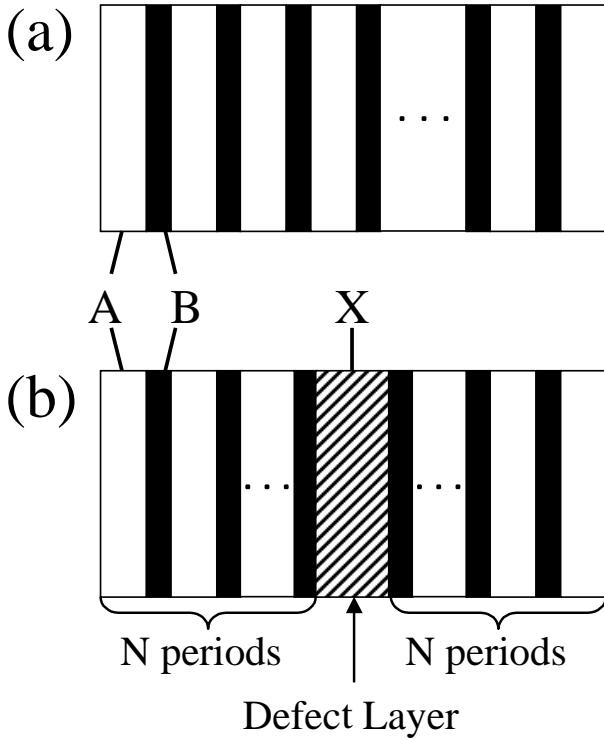


Fig. 1. Model of 1-D PC structures without defects (a) and with a defect (b).

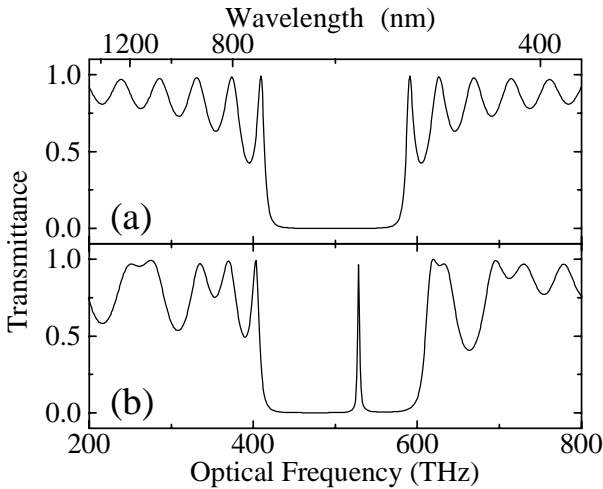


Fig. 2. Calculated transmission spectra of the 1-D PCs without defects (a) and with a defect (b).

propagating through the 1-D PCs is interesting since the electric field of light in photonic crystals corresponds to wave functions of electrons in normal crystals. We carried out the phase-sensitive detection of light propagating through the above 1-D PCs with and without defects using a white-light Michelson interferometer.

2.1 Time-domain measurement of linear propagation of light

We used a homemade white-light Michelson interferometer^{14,15)} in the phase-sensitive detection of light propagating through the 1-D PCs in the linear regime. The input light source was a normal incandescent lamp. The white light from the lamp was guided to a vibration-isolated bench

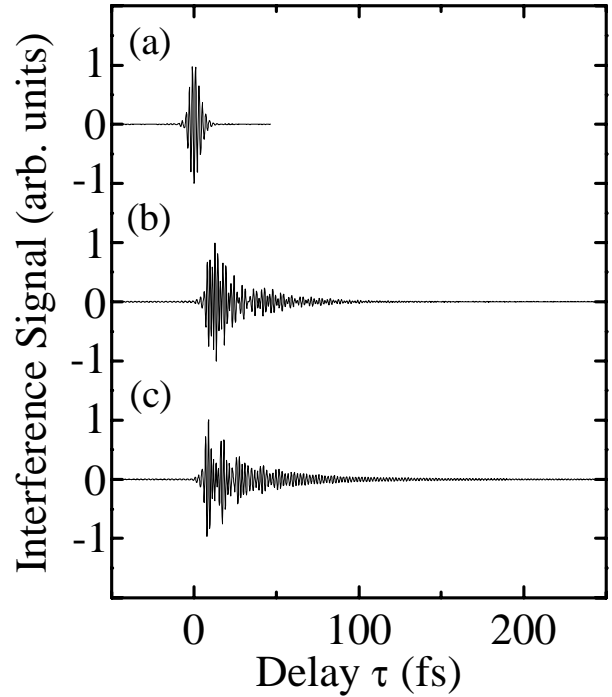


Fig. 3. Interferograms obtained by the Michelson interferometer. Autocorrelation, $C_A(\tau)$, of the input white light (a), and cross-correlation, $C_C(\tau)$, between the input white light and the transmitted light through the 1-D PCs without defects (b) and with a defect (c).

through a multimode optical fiber. In this experiment, we measured two kinds of interferograms: one is the autocorrelation, $C_A(\tau) = \langle E_{in}^*(t)E_{in}(t + \tau) \rangle$, of the input light, E_{in} , and the other is the cross-correlation, $C_C(\tau) = \langle E_{in}^*(t)E_{out}(t + \tau) \rangle$, between the input light and the light transmitted through the 1-D PC, E_{out} , where τ is the delay time or the path-length difference between the two arms of the interferometer.

In the linear regime, the following relation exists:

$$E_{out}(t) = \int_{-\infty}^t dt' h(t - t') E_{in}(t'), \quad (1)$$

where $h(t)$ is the response function of the 1-D PC. Inserting eq. (1) into $C_C(\tau)$, we obtain

$$C_C(\tau) = \int_{-\infty}^{\tau} d\tau' h(\tau - \tau') C_A(\tau'). \quad (2)$$

By comparing eqs. (1) and (2), we see that the relationship between $E_{in}(t)$ and $E_{out}(t)$ is exactly the same as that between $C_A(\tau)$ and $C_C(\tau)$. Therefore, we can say that if the waveform of the input light pulse is the autocorrelation, $C_A(\tau)$, then the waveform of the output light pulse is the cross-correlation, $C_C(\tau)$. That is, in the linear regime, using a white-light Michelson interferometer, we can observe the deformation of ultrashort light pulses by transmission through the 1-D PCs without using ultrashort pulse lasers.

The interferograms measured by the interferometer are shown in Fig. 3, where (a) is the autocorrelation, $C_A(\tau)$, of the input white light, and (b) and (c) are the cross-correlation, $C_C(\tau)$, for the 1-D PC without defects and that for the 1-D PC with a defect, respectively. According to the linear response theory mentioned above, we can consider that Fig. 3(a) is the waveform of the input, and Figs. 3(b) and 3(c) are the waveforms of the light transmitted through the 1-D PC without defects and the 1-D PC with a defect, respectively. This shows

that a 6 fs (FWHM) light pulse as shown in Fig. 3(a) is broadened by the passage through the 1-D PCs, and in Fig. 3(c) the trailing edge of the pulse is elongated more than that in Fig. 3(b) by the localization of the defect mode around the defect layer. Full information on the input and the transmitted light field enables us to obtain the complex transmission coefficients of the 1-D PCs.¹⁶⁾

2.2 Complex transmission coefficient of the 1-D PC

The photonic band structure in colloidal crystals was measured using a modified Mach-Zehnder interferometer by Tarhan *et al.*¹⁷⁾ In their measurement, the phase shift by the passage through a photonic crystal at a certain wavelength was derived by analyzing the interferometer fringe pattern. Then, a dispersion curve was obtained by changing the wavelength of the laser light source. In the present case, however, the complex transmission coefficient for a wide spectral region can be obtained simply by Fourier transformation of the measured interferograms as follows.

By Fourier transformation of eq. (1), we obtain

$$E_{\text{out}}(\omega) = t(\omega)E_{\text{in}}(\omega), \quad (3)$$

where $E_{\text{in}}(\omega)$ and $E_{\text{out}}(\omega)$ are the Fourier transforms of input light field, $E_{\text{in}}(t)$, and output light field, $E_{\text{out}}(t)$, respectively, and $t(\omega)$, which is called the complex transmission coefficient, is the Fourier transform of the impulse response function, $h(t)$. The Fourier transformation of eq. (2) yields a relation similar to eq. (3):

$$C_C(\omega) = t(\omega)C_A(\omega), \quad (4)$$

where $C_A(\omega)$ and $C_C(\omega)$ are the Fourier transforms of the autocorrelation, $C_A(\tau)$, and the cross-correlation, $C_C(\tau)$, respectively. Using these relations, we can obtain the complex transmission coefficient from the measured autocorrelation and cross-correlation interferograms. The complex transmission coefficient is written as

$$t(\omega) = |t(\omega)| \exp\{i\phi(\omega)\}, \quad (5)$$

where $|t(\omega)|$ is the amplitude transmission spectrum, and $\phi(\omega)$ is the phase difference between the input light and the transmitted light, which is called the phase spectrum.¹⁶⁾

Figure 4 shows the transmission and the phase spectra for 1-D PCs without defects (a) and with a defect (b), where solid curves are obtained by Fourier transformation of the measured interferograms and dashed curves are the transmission spectra obtained using a conventional grating spectrometer. The transmission spectra obtained by the two methods agree fairly well and reproduce the characteristic features of the theoretical transmission curves shown in Fig. 2. This proves the reliability of our interferometric measurements. The theoretically obtained phase spectra using the method of characteristic matrices are shown in Fig. 4 by dotted curves. Although the measured phase spectra in the band-gap region are noisy because of the extremely low transmission in this region, the key features of the theoretical curves are observed in the measured phase spectra.

The transmission and the phase spectra can be explained as follows: The transmission spectra reflect the density of photon modes in the photonic crystals. In the region of the photonic band gap, the incident light beam does not have any modes to couple with in the 1-D PCs; therefore, the light

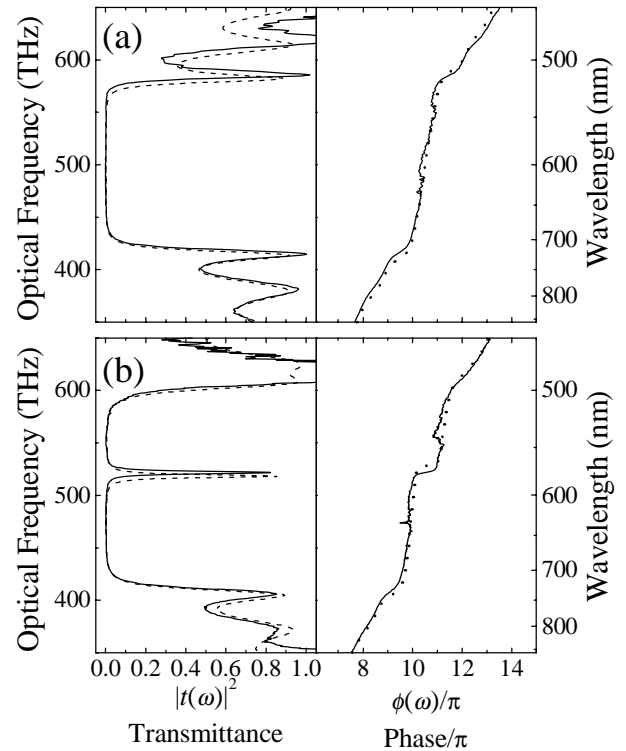


Fig. 4. Transmission spectra and phase spectra for 1-D PCs without defects (a) and with a defect (b). Solid curves are obtained by Fourier transformation of the measured interferograms, and dashed curves are obtained by a conventional grating spectrometer. The calculated phase spectra are shown by dotted curves.

beam cannot propagate into the crystal, but is totally reflected back. However, by the introduction of the defect layer, a defect level is created in the band-gap region. In this case, the incident beam couples with the defect mode and is transmitted through the crystal. This is represented by the sharp transmission peak shown in Fig. 4(b). On the other hand, the phase spectra correspond to the dispersion curves of the photonic crystals. The phase increases by π at the transmission peak, as shown in Fig. 4(b). This means that a new resonant mode is created at the frequency. The position of the defect mode can be controlled freely by changing the refractive index and/or the thickness of the defect layer.

2.3 Enhancement of light intensity at the defect layer

The 1-D PC with a defect is considered to be a microcavity where the light field of the resonant mode, or the defect mode, is localized around the defect layer. The field pattern of the resonant mode in the 1-D PC can be calculated using the method of characteristic matrices, and is shown in Fig. 5 for the 1-D PC with a structural defect shown in Fig. 1(b). If all the layers are transparent, light intensity at the defect layer is enhanced from the input intensity by a factor of $(n_B/n_A)^{2N}/2$, where N is the number of periods of A and B bilayers on each side of the defect layer.¹³⁾ Since $n_B/n_A = 1.6$ for the stacks of SiO_2 and TiO_2 , we can obtain an intensity enhancement of the order of 10^2 and 10^4 for $N = 5$ and $N = 10$, respectively. This fact leads to the expectation that the effective optical nonlinearity of the material at the defect layer can be enhanced in the 1-D PC with a structural defect. Although the intensity enhancement is caused by the high Q value of

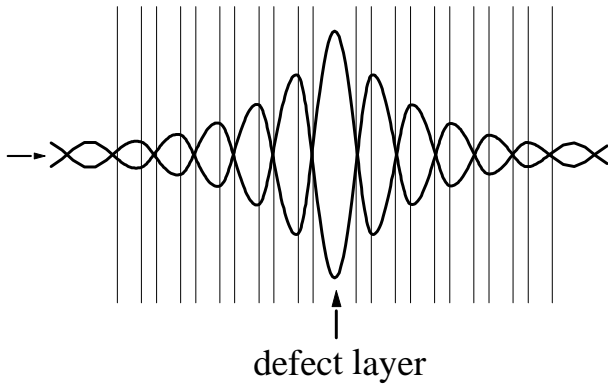


Fig. 5. Calculated field pattern of light at the frequency of the transmission peak of the 1-D PC with a defect.

the resonant mode, the decay time of the resonant mode is very short, of the order of 100 fs, as can be seen from Fig. 3, because of the small thickness of the 1-D PC structure. This implies that we can expect sub-picosecond time response using the 1-D PC with a structural defect, if an appropriate nonlinear material is used as the defect layer.

3. Nonlinear Optical Effect in 1-D PCs with a Defect

In the previous sections, we discussed the linear optical properties of 1-D PC structures where the material of each layer is assumed to be nonabsorptive. In the following, however, we discuss 1-D PC structures with a defect layer where the material of the defect layer is absorptive. Pure absorptive nonlinearity can be justified, assuming that the defect level wavelength falls in the central region of the absorption band, and that the dispersive contribution is much smaller than the absorptive one in this region. This point is in contrast to some reported cases of nonlinear Fabry-Perot etalons,^{10,12)} where the major contribution to the nonlinear transmittance change is thought to be dispersive nonlinearity. We chose absorptive nonlinearity because it can be induced by much smaller light intensity than the case of dispersive nonlinearity.

Previously, we analyzed the optical properties of 1-D PCs with a defect where the material of the defect layer is assumed to be purely absorptive.¹³⁾ According to the analysis, the transmittance, T , at the transmission peak of the defect level is expressed as

$$T = \frac{4}{\left[2 + \frac{\pi\kappa}{n_X} \left(\frac{n_B}{n_A} \right)^{2N} \right]^2}, \quad (6)$$

where n_A , n_B and n_X are the refractive indices of layers A, B and the defect layer, respectively, κ is the extinction coefficient of the defect layer, and N is the number of periods of A and B bilayers on each side of the defect layer. The intensity enhancement factor, G , at the center defect layer is given by using the transmittance, T , as

$$G = \frac{T}{2} \left(\frac{n_B}{n_A} \right)^{2N}. \quad (7)$$

Here, it is assumed that N is sufficiently large so that

$$(n_B/n_A)^N \gg 1, \quad (8)$$

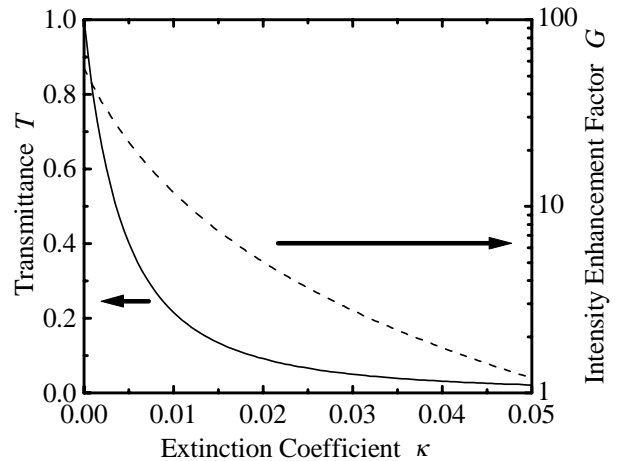


Fig. 6. Dependence of the transmittance of transmission peak, T (solid curve), and the intensity enhancement factor, G (dashed curve), on the extinction coefficient, κ .

and that

$$n_X \gg \kappa. \quad (9)$$

For the 1-D PC with periodical stacks of SiO_2 and TiO_2 , if $N = 5$, then, the value of $(n_B/n_A)^N$ is $1.6^5 \sim 10$.

For samples with finite absorption, both the transmittance, T , and the intensity enhancement factor, G , are considerably suppressed by the absorption in the defect layer. Figure 6 shows the dependence of T and G on the extinction coefficient κ of the defect layer. Since the nonlinear susceptibility is expected to be proportional to the density of the absorption center, i.e., proportional to the extinction coefficient κ , it is necessary to optimize κ in order to obtain the maximum enhancement of the effective optical nonlinearity for a fixed value of N .

3.1 Absorption saturation

In order to observe absorption saturation, we fabricated a sample with a nonlinear optical material as the defect layer in a 1-D PC structure. The defect layer of the sample is a spin-coated polyvinyl alcohol film doped with oxazine 1 dye molecules. This film was sandwiched between the two 1-D PCs with the same structure, which are composed of five period quarter-wave stacks of SiO_2 and TiO_2 . The overall structure is the same as that shown in Fig. 1(b). The optical thickness of both layers A and B is $640 \text{ nm}/4$, and that of the defect layer was controlled by applying pressure to the glass substrates on both sides of the 1-D PC before the polymer film was completely dry. Figure 7 shows the transmission spectrum of the 1-D PC with a defect thus made. The transmittance of the transmission peak at 620 nm is reduced to about 50% by the absorption of oxazine 1. According to the curve shown in Fig. 6, this reduction of transmittance corresponds to the defect layer extinction coefficient κ of 3×10^{-3} .

As a reference sample, a naked polyvinyl alcohol film doped with oxazine 1 was also prepared. The transmittance of the naked film was controlled to be almost equal to the peak transmittance of the 1-D PC at 620 nm , 50%. Absorption saturation of the two samples was measured using nanosecond laser pulses at 620 nm . Comparison of the saturation behavior of the films with and without the PC structure over five

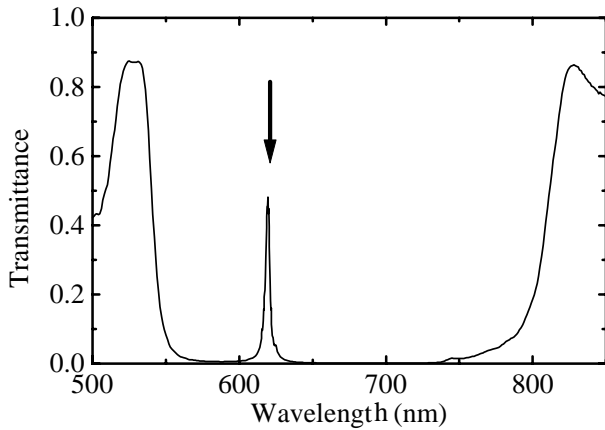


Fig. 7. Transmission spectrum of the 1-D PC with a defect. The defect layer is a polyvinyl alcohol film doped with oxazine 1. Arrow indicates the excitation wavelength, 620 nm.

orders of magnitude is shown in Fig. 8.¹⁸⁾ This shows that the saturation intensity of the 1-D PC is reduced by a factor of 20 compared with that of the naked film. This result is consistent with the theoretically obtained value of intensity enhancement factor, $G = 30$, for $\kappa = 3 \times 10^{-3}$ of the defect layer.

3.2 Degenerate four-wave mixing

The enhancement of light intensity at the defect layer in the 1-D PC was experimentally verified by the observation of absorption saturation. Although this is a direct observation of the enhancement of light intensity in the 1-D PC with a defect, our main concern is the enhancement of the nonlinear optical effect and its application as future nonlinear optical devices. Therefore, the efficiency of degenerate four-wave mixing (DFWM) in the 1-D PC with a defect was compared with that in a naked film without the PC structure. Signal processing by DFWM is considered to be one of the major possible applications of thin-film nonlinear material, where three beams with wave vectors \mathbf{k}_1 , \mathbf{k}_2 and \mathbf{k}_3 are incident on a sample, and a signal beam with a wave vector $\mathbf{k}_1 + \mathbf{k}_2 - \mathbf{k}_3$ is diffracted from the sample.

In this experiment, the second harmonic of a Q-switched YAG laser with a pulse width 5 ns at 532 nm was used as the excitation source for convenience. We fabricated a 1-D PC where the defect layer is a spin-coated polyvinyl alcohol film doped with eosin Y. The optical thickness of each layer of five period bilayers of SiO₂ and TiO₂ on both sides of the defect layer was 488 nm/4. The wavelength of the second harmonic, 532 nm, of the Q-switched YAG laser is well within the band-gap region of the 1-D PC. The transmission spectrum of the 1-D PC with a defect is shown in Fig. 9. Several defect levels are created in the band-gap region, since the optical thickness of the defect layer is larger than half-wavelength, 488 nm/2. From the spectrum shown in Fig. 9, the optical thickness and the extinction coefficient κ of the defect layer are estimated to be about 5×488 nm and 2×10^{-2} , respectively. One of the transmission peaks was controlled to be at the excitation wavelength, 532 nm, as shown by an arrow in Fig. 9. As a reference sample, we prepared a naked polyvinyl alcohol film doped with eosin Y on a glass substrate without the 1-D PC structure. The extinction coefficient of the naked film was controlled to be the same as that of the defect layer in the 1-D PC, 2×10^{-2} , which corresponds to the naked film transmis-

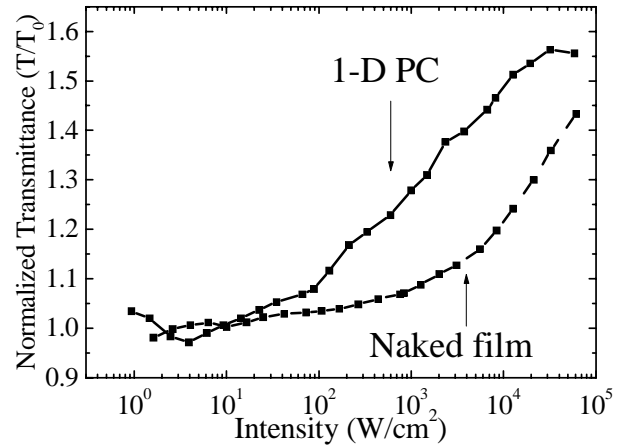


Fig. 8. Dependence of normalized transmittance of transmission peak on the input light intensity for the 1-D PC with a defect (solid curve) and the naked reference film without 1-D PC structure (dashed curve).

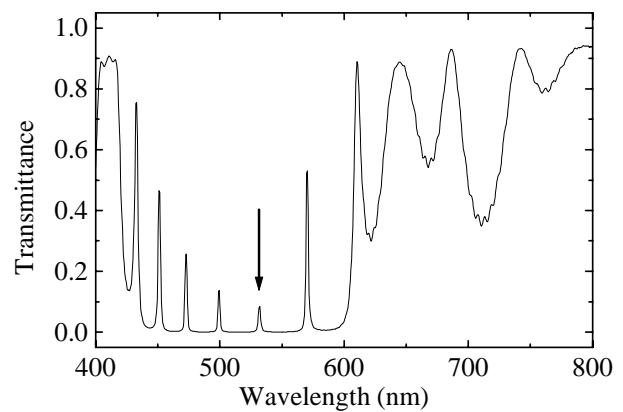


Fig. 9. Transmission spectrum of the 1-D PC with a defect. The defect layer is a polyvinyl alcohol film doped with eosin Y. Arrow indicates the excitation wavelength, 532 nm.

sion of 0.9. Since the wavelength of the transmission peak of the 1-D PC depends on the angle of incidence, we used box-CARS configuration^{19,20)} of DFWM where the angles of incidence of all the three excitation beams and the output beam were the same, 2°. According to our previous analysis,¹³⁾ the normalized DFWM generation efficiencies are expressed as

$$W_{1\text{-D PC}} = \frac{9}{16} \left(\frac{n_B}{n_A} \right)^{4N} T^3 (1 - \sqrt{T})^2, \quad (10)$$

for the 1-D PC with a defect, and

$$W_{\text{naked}} = \frac{1}{4} T (1 - T)^2, \quad (11)$$

for the naked film, where T is the transmittance of each sample. In the present experiment, $T = 0.1$ for the 1-D PC and $T = 0.9$ for the naked film; therefore, we obtain

$$W_{1\text{-D PC}} / W_{\text{naked}} = 1,300, \quad (12)$$

by the analysis.

The experimental result is shown in Fig. 10, where the DFWM signal intensities are compared between the 1-D PC and the naked film by changing the incident light intensity. Here the intensities of all the three incident beams were set to be almost the same. In both cases, the DFWM intensity has a

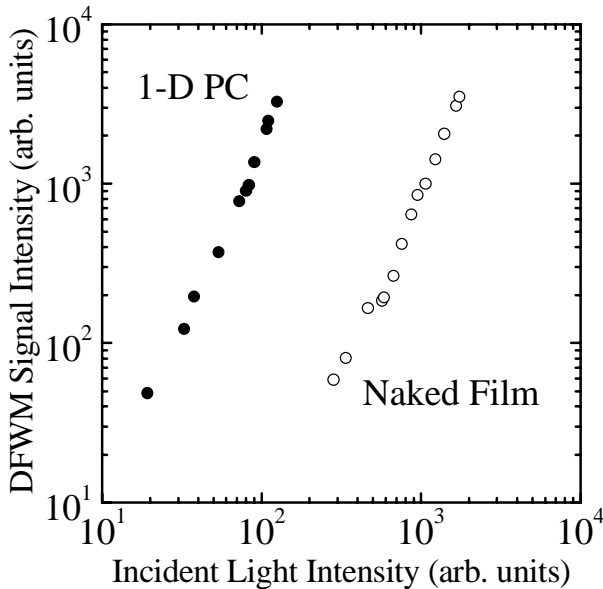


Fig. 10. Dependence of generated DFWM intensity on the incident light intensity for the 1-D PC with a defect (closed circle) and the naked reference film without 1-D PC structure (open circle).

cubic power dependence on the incident light intensity, as expected. The obtained enhancement of DFWM generation efficiency of the 1-D PC, 1,000, against the naked film is in good agreement with the theoretical prediction, 1,300. According to eqs. (10) and (11), for both the 1-D PC and the naked film, the normalized DFWM generation efficiency takes a maximum value around $T = 0.5$. If we compare the DFWM generation efficiencies between the 1-D PC and the naked film by setting $T = 0.5$ for both cases, the generation efficiency in the 1-D PC is larger by more than 2,000 times than that in the naked film.¹⁶⁾ However, if we reduce the extinction coefficient κ of the defect layer in the 1-D PC, light scattering by the residual optical imperfection in the defect layer obscures the DFWM signal. This is because multiple reflection of light in the 1-D PC enhances the scattering, especially when κ is small. It is necessary to improve the optical quality of 1-D PCs to make full use of the enhancement effect of the optical nonlinearity in 1-D PCs.

The nonlinear material in the defect layer of the present 1-D PC is a dye molecule which has a large oscillator strength and the nonlinearity is caused by the saturation of the resonant absorption; therefore, the defect layer itself has a large optical nonlinearity and the effective nonlinearity is further enhanced by the 1-D PC structure. Here, the response time of the 1-D PC is limited by the excited-state lifetime of the dye molecule, which is several nanoseconds. On the other hand, the cavity lifetime of the present 1-D PC is about 100 fs, as shown in Fig. 3(c); therefore, we can expect a sub-picosecond response time of a 1-D PC if the defect layer of the 1-D PC is made of nonlinear material with an ultrashort response time.

3.3 Phase-conjugated wave generation

Dye-doped polymer films are good media for phase conjugation optics and image processing.^{21,22)} Although the present 1-D PC has a slightly complicated structure, the total thickness is only a few micrometers. This point differs from ordinary nonlinear etalons used for bistability or optical switch-



Fig. 11. Obtained optical phase-conjugated image of "A" by the 1-D PC.

ing. Therefore, the present 1-D PC can be used to form an optical phase-conjugated image.

For the demonstration of image construction, a cw Ar laser at 514.5 nm was more convenient as the excitation source. The defect layer in this case was a polyvinyl alcohol film doped with methyl orange. The dielectric stacks on both sides of the defect layer were the same as these in the above-mentioned DFWM experiment. Since the wavelength of the transmission peak depends on the angle of incidence on the 1-D PC, optical systems are aligned such that all the three incident beams and the phase-conjugated beam have the same angle of incidence. The acceptance angle of the transmission peak of the 1-D PC was about 80 mrad; therefore, the beam divergence of the image probe beam was limited by this angle. The incident beams were focused on the 1-D PC to a spot diameter of about 1 mm, and the power of each incident beam was 2–3 mW. Here, the pump beams were longitudinally polarized, and the probe beam was transversely polarized. The transversely polarized phase-conjugated image was detected by a digital camera through a polarizing plate which transmitted the transverse polarization and eliminated the scattered light of the pump beams. Figure 11 shows the formed phase-conjugated image of "A" by the present 1-D PC. Because of the residual optical imperfection of the defect layer in the 1-D PC, the formed image may not be so clear. However, it was apparently shown that 1-D PC structures can be used for phase conjugation optics and image processing. For better image construction, better optical quality is required for the defect layer, and better optical contact between the defect layer and the neighboring periodical dielectric stacks is also indispensable.

4. Conclusion

We investigated the optical linear properties of 1-D PCs using a white-light Michelson interferometer and obtained the photonic band structure and the dispersion relation. Moreover, we studied the enhancement of optical nonlinearity using 1-D PC structures, and observed a 1,000 times enhancement of the DFWM generation efficiency of the 1-D PC, com-

pared with the naked film. Finally, the 1-D PC was successfully used to form an optical phase-conjugated image. For better optical quality and stability, and shorter response time, we are currently investigating the possibility of using other materials as the defect layer. The 1-D PC structures may be one of the key devices in future optical processing.

- 1) *Photonic Band Gaps and Localization*, ed. C. M. Soukoulis (Plenum, New York, 1993).
- 2) *Photonic Band Gap Materials*, ed. C. M. Soukoulis (Kluwer Academic Publishers, Dordrecht, 1996).
- 3) *Microcavities and Photonic Bandgaps: Physics and Applications*, ed. J. Rarity and C. Weisbuch (Kluwer Academic Publishers, Dordrecht, 1996).
- 4) E. Yablonovitch: *Phys. Rev. Lett.* **58** (1987) 2059.
- 5) H. Hirayama, T. Hamano and Y. Aoyagi: *Appl. Phys. Lett.* **69** (1996) 791.
- 6) H. Benisty: *J. Appl. Phys.* **79** (1996) 7483.
- 7) R. Shimano, S. Inouye, M. Kuwata-Gonokami, T. Nakamura, M. Yamanishi and I. Ogura: *Jpn. J. Appl. Phys.* **34** (1995) L817.
- 8) R. Buhleier, V. Bardinal, J. H. Collet, C. Fontaine, M. Hubner and J. Kuhl: *Appl. Phys. Lett.* **69** (1996) 2240.
- 9) H. M. Gibbs, S. L. McCall and T. N. C. Venkatesan: *Phys. Rev. Lett.* **36** (1976) 1135.
- 10) H. M. Gibbs, S. L. McCall, T. N. C. Venkatesan, A. C. Gossard, A. Passner and W. Wiegmann: *Appl. Phys. Lett.* **35** (1979) 451.
- 11) H. M. Gibbs: *Optical Bistability: Controlling Light with Light* (Academic Press, Orlando, 1985).
- 12) R. Quintero-Torres and M. Thakur: *Appl. Phys. Lett.* **66** (1995) 1310.
- 13) T. Hattori, N. Tsurumachi and H. Nakatsuka: *J. Opt. Soc. Am. B* **14** (1997) 348.
- 14) N. Tsurumachi, T. Fuji, S. Kawato, T. Hattori and H. Nakatsuka: *Opt. Lett.* **19** (1994) 1867.
- 15) T. Fuji, M. Miyata, S. Kawato, T. Hattori and H. Nakatsuka: *J. Opt. Soc. Am. B* **14** (1997) 1074.
- 16) T. Hattori, N. Tsurumachi, S. Kawato and H. Nakatsuka: *Phys. Rev. B* **50** (1994) 4220.
- 17) I. I. Tarhan, M. P. Zinkin and G. H. Watson: *Opt. Lett.* **20** (1995) 1571.
- 18) T. Hattori, N. Tsurumachi, N. Muroi, H. Nakatsuka and E. Ogino: *Prog. Cryst. Growth & Charact.* **33** (1996) 183.
- 19) L. Yang, R. Dorsinville, Q. Z. Wang, W. K. Zou, P. P. Ho, N. L. Yang, R. R. Alfano, R. Zamboni, R. Danieli, G. Ruani and C. Taliani: *J. Opt. Soc. Am. B* **6** (1989) 753.
- 20) W. Du, X. Zhang, K. Chen, Z. Lu, Y. Zheng and J. Wu: *Opt. Commun.* **84** (1991) 205.
- 21) Y. Silberberg and I. Bar-Joseph: *Opt. Commun.* **39** (1981) 265.
- 22) T. Todorov, L. Nikolova, N. Tomova and V. Dragostinova: *IEEE J. Quantum Electron.* **22** (1986) 1262.